

Phase-shift time-stepping for reverse-time migration: the Marmousi data experience

Ben D. Wards, Gary F. Margrave, and Michael P. Lamoureaux*

ABSTRACT

As a result of the numerical performance of finite-difference operators, reverse-time migration (RTM) produces images which are typically low frequency or require large computational resources. We consider an alternative to wavefield propagation with finite differences, a two-way high-fidelity time-stepping equation based on the Fourier transform which is exact for homogeneous media if an aliasing condition is met. The technique is adapted to variable velocity using a localized Fourier transform (Gabor transform). The feasibility of using the time-stepping equation for RTM is demonstrated by studying its stability properties, and by migrating the Marmousi data set. We show that a high frequency wavefield can be time-stepped with no loss of frequency content and with a much larger time step than is commonly used.

INTRODUCTION

Reverse-time migration (Baysal et al., 1983; McMechan, 1983) is a powerful depth migration algorithm. It is capable of imaging reflectors using overturned waves and multiples. However, as a result of the sampling requirements, processing seismic surveys will either require harsh filtering to remove higher frequency data, or they will require long run times even with a cluster of computers. The fine sampling requirements occur because finite-difference operators propagate high frequencies with an incorrect dispersion relation. An example of the impressive performance, yet low frequency response, is given in Jones et al. (2007).

We propose an alternative time-stepping equation that does not use finite differences. Our equation can time step a wavefield using a coarser time step because the spatial derivatives in the wave equation are computed exactly in the Fourier domain and so do not suffer from dispersion at high frequencies. As a result, the sampling requirements are better than propagating with finite differences. Moreover, since our solution is based on evaluating the exact solution to the wave equation it does not suffer from numerical dispersion associated with either pseudospectral or finite difference methods. The fundamental limitation on the time step size in our method arises from a temporal aliasing condition, which we derive. The accuracy and stability properties are demonstrated by comparing solutions of the time-stepping equation to finite-difference solutions. We extend our method to variable velocity by replacing the global Fourier transform with a local Gabor transform using localizing windows within which a locally homogeneous solution is computed.

*POTSI, Dept. of Mathematics and Statistics, University of Calgary

TIME STEPPING BY A PHASE-SHIFT INTEGRAL: THEORY

The following conventions are used for the forward and inverse Fourier transform of the function $\varphi : \mathbb{R}^2 \rightarrow \mathbb{R}$,

$$\hat{\varphi}(\vec{k}) = \mathcal{F}(\varphi) = \int_{\mathbb{R}^2} e^{2\pi i \vec{x} \cdot \vec{k}} \varphi(\vec{x}) dx dz,$$

and

$$\hat{\varphi}(\vec{x}) = \mathcal{F}^{-1}(\hat{\varphi}) = \int_{\mathbb{R}^2} e^{-2\pi i \vec{x} \cdot \vec{k}} \hat{\varphi}(\vec{k}) dk_x dk_z,$$

where \mathbb{R} is the real line, $i = \sqrt{-1}$, $\vec{x} \in \mathbb{R}^2$, \vec{k} is the Fourier domain coordinate conjugate to \vec{x} . The symbols \mathcal{F} , and \mathcal{F}^{-1} are used to denote the forward and inverse Fourier transforms as abstract operators, respectively.

Wavefield continuation migration methods recursively extrapolate the recorded wavefield downward in depth. In contrast, RTM back propagates the recorded wavefield in time. This is typically done by finite-differencing the two-way wave equation. As an alternative to finite-differencing the wave equation, our time-stepping equation is formulated by phase-shifting the Fourier transform of the wavefield by a cosine operator. The time-stepping equation is based on an exact solution of the constant velocity wave equation,

$$\frac{\partial^2 U}{\partial t^2} = c^2 \left(\frac{\partial^2 U}{\partial x^2} + \frac{\partial^2 U}{\partial z^2} \right), \quad (1)$$

where $U(t, x, z)$ is the amplitude of the wave at the point (t, x, z) , x is the lateral coordinate, z is the depth coordinate, t is the time coordinate, $\partial^2 U / \partial t^2$ is, for example, the second order partial derivative of the wavefield with respect to the time coordinate, and c , a constant, is the speed of propagation. Assume $(x, z) \in \mathbb{R}^2$ and $t > 0$.

Applying the Fourier transform over the spatial dimensions $\vec{x} = (x, z)$ to both sides of equation (1), reduces it to a collection of ordinary differential equations,

$$\frac{\partial^2 \hat{U}}{\partial t^2} = -(2\pi)^2 c^2 (k_x^2 + k_z^2) \hat{U}, \quad (2)$$

where

$$\hat{U} = \hat{U}(t, k_x, k_z) = \int_{\mathbb{R}^2} U(t, x, z) e^{2\pi i \vec{x} \cdot \vec{k}} dx dz, \quad (3)$$

and $\vec{k} = (k_x, k_z)$ are the wavenumbers which correspond to the coordinates $\vec{x} = (x, z)$. Equation (2), unlike equation (1), is not valid when the wave speed depends upon either spatial coordinates. When $\vec{k} \neq 0$, equation (2) has the general solution,

$$\hat{U}(t, k_x, k_z) = A(k_x, k_z) \cos(2\pi\omega(k_x, k_z)t) + B(k_x, k_z) \sin(2\pi\omega(k_x, k_z)t), \quad (4)$$

where $A(k_x, k_z)$ and $B(k_x, k_z)$ are dependent on the initial conditions, and wavenumber dependent frequency ω is determined from the dispersion relation

$$\omega(k_x, k_z) = c\sqrt{k_x^2 + k_z^2}. \quad (5)$$

After the functions A and B are specified, the space domain solution may be calculated by taking an inverse Fourier transform. Subject to the initial conditions $U(0, x, z) = f(x, z)$ and $U(-\Delta t, x, z) = g(x, z)$, the functions are $A(k_x, k_z) = \hat{f}(k_x, k_z) = \hat{U}(0, k_x, k_z)$ and $B(k_x, k_z) \sin(2\pi\omega\Delta t) = \hat{f}(k_x, k_z) \cos(2\pi\omega\Delta t) - \hat{g}(k_x, k_z)$. The resulting exact solution of the constant velocity wave equation is

$$U(\Delta t, x, z) = -U(-\Delta t, x, z) + 2\mathcal{F}^{-1}[\cos(2\pi\omega(k_x, k_z)\Delta t)\mathcal{F}[U(0, x, z)]], \quad (6)$$

where \mathcal{F} and \mathcal{F}^{-1} are the forward and inverse 2D Fourier transform, respectively. The fast Fourier transform can be employed because the phase shift operator, $\cos(2\pi\omega(k_x, k_z)\Delta t)$, is independent of the spatial coordinate \vec{x} .

The second-order time and second-order space finite-difference solution of the wave equation can be derived formally from equation (6) by replacing the cosine function by its second order power series expansion. Thus equation (6) clearly generalizes explicit finite difference schemes and, for homogeneous media, is superior.

To demonstrate the effectiveness of recursively using equation (6) for wavefield propagation, a minimum phase wavelet is stepped forward in time. The minimum phase wavelet is injected at the center point of the model at the start of propagation. Figure 1 shows the propagation of a minimum phase wavelet using the phase-shift time stepper and also with conventional second-order finite differencing. In spite of a much smaller time step, the finite-difference solution is still noisy.

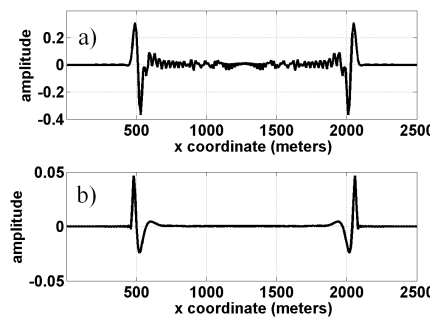


FIG. 1. Cross section, through center of the model, of the response to a minimum phase wavelet injected at the center of the model. (a) Using finite differences with $\Delta t = 0.0001$. (b) Using phase-shift time-stepping equation with $\Delta t = 0.001$. The finite-difference time stepper took 10 times as long to execute.

STABILITY

While our result is exact for constant velocity, with sampled data the size of the time step is limited by aliasing considerations. Equation (6) takes the wavefield at two distinct times with spatial sampling rate Δx and generates a new wavefield at a future time.

The wavenumber which corresponds to the greatest frequency occurs when $(k_x, k_z) = (\pm \frac{\pi}{\Delta x}, \pm \frac{\pi}{\Delta x})$, the Nyquist wavenumbers. By the dispersion relation, the maximum wavenumber generates a frequency $\omega = \pi c\sqrt{2}/\Delta x$. Since the wavefield is sampled in time at rate Δt , the Nyquist frequency is $\omega = \pi/\Delta t$. Thus the Courant-Friedrichs-Levy (CFL) number $r = \Delta t c/\Delta x$ must satisfy the inequality $r < 1/\sqrt{2}$ to avoid aliasing. This limitation on the step size is far less restrictive than that usually encountered in finite-difference time stepping. Figure 2 shows how stability breaks down $r = 1/\sqrt{2}$.

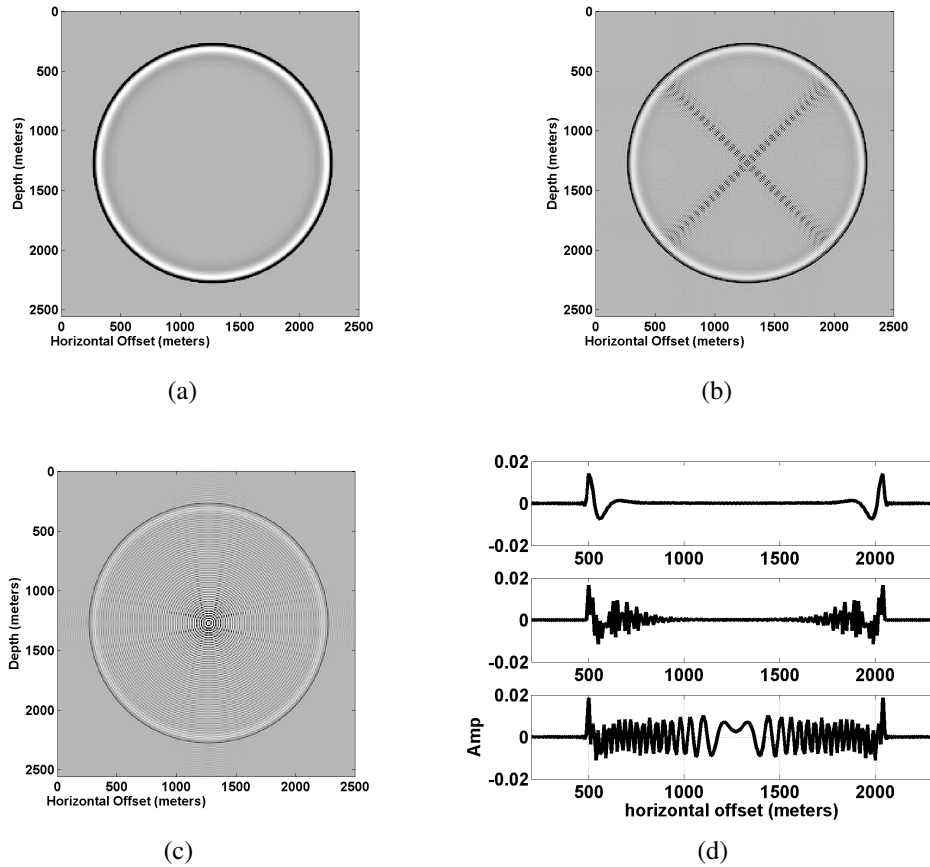


FIG. 2. Cross-sectional view of the response to a minimum phase wavelet injected at the center of a constant velocity model and forward propagated for various values of the CFL number r . When $r > 1$ aliasing occurs in the model and the model is unstable. From top to bottom the CFL number $r = 0.60 \leq 0.71$, $r = 0.80 \leq 0.71$, and $r = 1.00 \leq 0.71$, respectively.

TIME STEPPING IN A VARIABLE-VELOCITY MEDIUM

The variable velocity acoustic wave equation is

$$\frac{\partial^2 U}{\partial t^2} = v^2(x, z) \left(\frac{\partial^2 U}{\partial x^2} + \frac{\partial^2 U}{\partial z^2} \right), \quad (7)$$

where $v(x, z)$ is the spatially dependent velocity. We now adapt equation (6), which propagates an acoustic wavefield exactly in a constant velocity medium, to propagate approximately in a variable velocity medium. Equation (7) has a local property which means that the wavefield $U(t, \vec{x})$ only depends on the wavefield in its backwards light cone. As

a result, it can be argued that the right hand side of equation (7), $v^2(\vec{x})(U_{xx} + U_{zz})$, can be approximated locally near \vec{x}_0 by the solution to the frozen equation $v^2(\vec{x}_0)(U_{xx} + U_{zz})$. This means that by simply replacing the constant velocity appearing in the dispersion relation in equation (6) by the variable velocity, we have an approximate solution

$$U(\Delta t, \vec{x}) = -U(-\Delta t, \vec{x}) + 2\mathcal{F}^{-1} \left[\cos \left(2\pi v(\vec{x}) \|\vec{k}\| \Delta t \right) \mathcal{F} [U(0, \vec{x})] \right]. \quad (8)$$

This is the freezing argument. It appears often in the literature in the context of elliptic partial differential equations e.g. Stein (1993). Such solutions are often called locally homogeneous approximations. While it is not a mathematically precise argument, it does provide an accurate approximation.

Equation (6) can be computed efficiently because at every time step two 2-dimensional fast Fourier transforms (FFT) and one matrix multiplication are computed. In contrast, for equation (8) the FFT can not be used so that the numerical complexity at each time step is $n_z^2 n_x^2$ versus $n_x \log(n_x) n_z \log(n_z)$ if the FFT could be used where n_x, n_z are the number of points used to discretize the x, z variable, respectively.

THE GABOR TRANSFORM

The Fourier transform has been used extensively in seismic signal processing as a method of filtering, and for wavefield continuation migrations (Gazdag, 1978; Stolt, 1978). However, seismic signals change character over space and time, requiring a time variant or space variant filtering (Margrave, 1998). For wavefield continuation migrations, the Fourier transform methods lose their efficiency as the velocity model becomes more complex. As an alternative to the Fourier transform or as a generalization of it, the Gabor transform has been used successfully to deal with the nonstationary character of seismic signals. It was first proposed by windowing a signal with a space shifted Gaussian function (Gabor, 1946). The Gabor transform has been used successively in seismic imaging to implement nonstationary filters. For example, Margrave et al. (2005) proposed Gabor deconvolution which corrects the data for anelastic attenuation. While Margrave and Lamoureux (2002), Ma and Margrave (2008), and Grossman et al. (2002) have proposed highly accurate Gabor depth imaging algorithms.

To solve the wave equation in a variable velocity medium, the velocity function is approximated by using a partition of unity (POU). A POU is a smooth decomposition of unity, e.g. $1(\vec{x}) = \sum_j \Omega_j(\vec{x})$, where the $\Omega_j(\vec{x})$ are smooth functions. Given a particular mean error ϵ , there exists a POU $\{\Omega_j(\vec{x}), \vec{x} \in \mathbb{R}^2, j \in J\}$ and a collection of reference velocities $\{v_j, j \in J\}$ so that $\|\sum_{j \in J} v_j \Omega_j(\vec{x}) - V(\vec{x})\| < \epsilon$, where $|\vec{x}| = \sqrt{x^2 + z^2}$, J is the indexing set, and $\Omega_j(\vec{x})$ is a continuous function of \vec{x} .

Suppose that the velocity $V : \mathbb{R}^2 \rightarrow \mathbb{R}$ and $I_j : \mathbb{R}^2 \rightarrow \{0, 1\}, j \in J$ such that $\sum_{j \in J} I_j = 1$. and $\|\sum_{j \in J} v_j I_j(\vec{x}) - V(\vec{x})\| < \epsilon$. Suppose that $w : \mathbb{R}^2 \rightarrow \mathbb{R}$ is a smooth function localized at $\vec{x} = 0$. For example, w could be a Gaussian function $\exp(-x^2/2\sigma^2)$ for

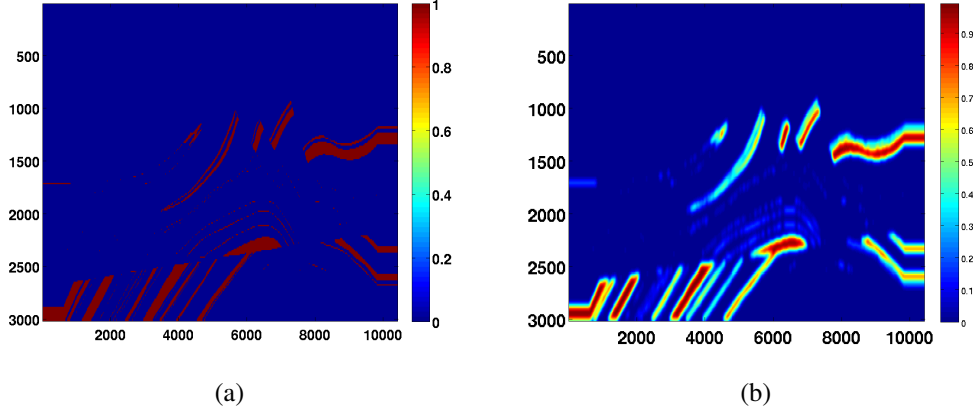


FIG. 3. (a) A non smooth window I_j used to migrate the Marmousi data set. (b) The corresponding smoothed window Ω_j .

a particular value of σ which determines the degree of smoothing. Then

$$\Omega_j = \frac{w * I_j}{\sum_{j \in J} w * I_j}, j \in J, \quad (9)$$

defines a POU. Figure is a single window used to migrate the Marmousi data set. The POU can be used to define a Gabor analysis and synthesis window pair. Let $g_i(\vec{x}) = \Omega_j^p(\vec{x})$ and $\gamma_i(\vec{x}) = \Omega_j^{1-p}(\vec{x})$ for any $p \in [0, 1]$. The functions $\{g_j, j \in J\}$ are called analysis windows, while the functions $\{\gamma_j, j \in J\}$ are called synthesis windows. The forward Gabor transform is defined by

$$V_g \psi_j(\vec{x}) = \mathcal{F}[g_j(\vec{x})\psi(\vec{x})]. \quad (10)$$

An inverse to the Gabor transform operating on the Gabor spectra $W(\vec{x}, j)$ is defined by

$$V_\gamma^{-1} W(\vec{x}, j) = \sum_j \gamma_j(\vec{x}) \mathcal{F}^{-1}[W(\vec{x}, j)], \quad (11)$$

hence

$$\begin{aligned} V_\gamma^{-1} V_g \psi_j(\vec{x}) &= \sum_j \gamma_j(\vec{x}) \mathcal{F}^{-1}[V_g \psi_j(\vec{x})] \\ &= \sum_j \gamma_j(\vec{x}) \mathcal{F}^{-1} \mathcal{F}[g_j(\vec{x})\psi(\vec{x})] \\ &= \sum_j \gamma_j(\vec{x}) g_j(\vec{x}) \psi(\vec{x}) \\ &= \sum_j \Omega_j(\vec{x}) \psi(\vec{x}) \\ &= \psi(\vec{x}). \end{aligned} \quad (12)$$

In general, the inverse to the Gabor transform is not unique, but the above definition is easy to compute and enjoys good numerical properties. For wavefield propagation the cases

$p = 0, 1$ turn out to be more interesting. This is because the cases $p \in (0, 1)$ take twice as long to compute as the cases $p = 0, 1$.

A Gabor multiplier is the Gabor transform equivalent of a Fourier transform filter. The Gabor spectrum is multiplied pointwise by a time-frequency or space-wavenumber filter. The inverse of the new spectrum is calculated to obtain the nonstationary filtered signal. Specifically, a Gabor multiplier, is the triple (g, γ, M) where for a function $\psi : \mathbb{R}^2 \rightarrow \mathbb{R}$, suitably defined, obeys the relation

$$M_{g,\gamma}\psi = V_\gamma^{-1}MV_g\psi. \quad (13)$$

In general, the action of the Gabor multiplier depends upon the windowing functions.

A FAST VARIABLE VELOCITY PSTS EQUATION

As mentioned previously, equation (8) is too numerically complex to be used directly for RTM. We use a Gabor windowing scheme to approximate it, and so the resulting operator is a Gabor multiplier. Equation (8) is a Fourier integral operator (Stein, 1993). Numerical computation of these operators is an active area of research (Candès et al., 2007).

The POU is used to window the wavefield into regions with approximate constant velocity. Each region is then propagated with a constant velocity v_j . The POU is used to window the wavefield into regions at each time step, and the combination of windowing and Fourier transformation converts equation (6) into

$$U(\Delta t, \vec{x}) = -U(-\Delta t, x, z) + \sum_{n=1}^N 2\mathcal{F}^{-1}[\cos(2\pi\omega_n\Delta t)\mathcal{F}[\Omega_n(x, z)U(0, x, z)]], \quad (14)$$

where $\omega_n(k_x, k_z) = v_n\sqrt{k_x^2 + k_z^2}$, $\Omega_n(x, z) = \Omega_n(z)$, and v_n is the velocity used for propagation in the n th window. In this case we have chosen $p = 0$. Choosing $p = 1$ or $p = 0$ produces nearly identical numerical results.

It is possible to write equation (14) as a Gabor multiplier. If $g_n = \Omega_n$, $\gamma_n = 1$, and $M(n, k_x, k_z) = \cos(2\pi\omega_n\Delta t)$, then

$$\begin{aligned} U(\Delta t, \vec{x}) &= -U(-\Delta t, x, z) + \\ &\quad \sum_{n=1}^N \gamma_n \mathcal{F}^{-1}M(n, k_x, k_z)\mathcal{F}[g_n U(0, x, z)], \\ &= -U(-\Delta t, x, z) + V_\gamma^{-1}MV_g U(t, x, z), \end{aligned} \quad (15)$$

CONSTRUCTING GABOR ANALYSIS WINDOWS

The computational complexity of the PSTS equation depends linearly on the number of reference velocities used to approximate the velocity model. Constructing accurate low order approximations makes for more accurate and numerically efficient phase shift time stepping algorithms.

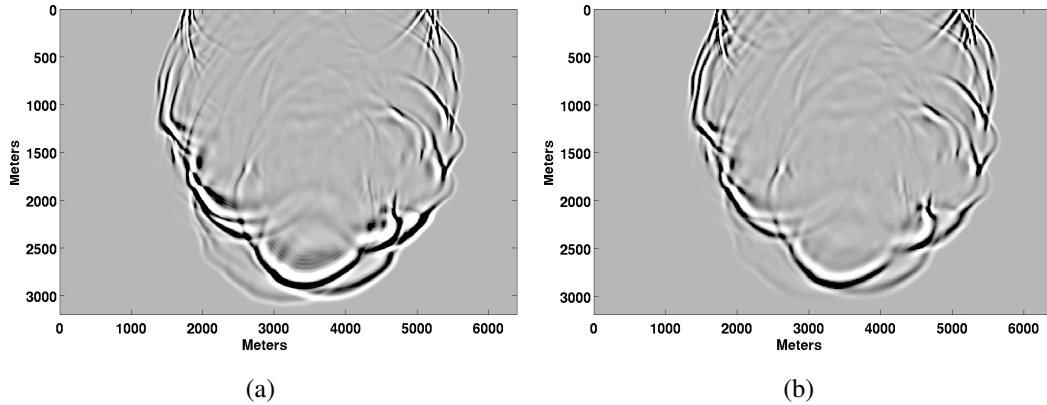


FIG. 4. On the left is a snapshot of the shotfield propagated by finite differencing the wave equation. On the right is the snapshot of the shotfield using PSTS for variable velocity.

We developed an iterative algorithm that chooses reference velocities based on minimizing the l^2 error, $\|v(x, z) - \sum_{j=1}^N v_j \Omega_j\|$, at each step in the iteration of the algorithm. Each iteration involves choosing a reference velocity. The algorithm can be broken down into a number of steps:

1. Suppose that the reference velocities $\{v_1, \dots, v_N\}$ have been chosen.
2. Calculate a histogram of $v(x, z)$ with a buffer removed around the reference velocities $\{v_1, \dots, v_N\}$.
3. Choose a few of the most frequently occurring velocity bins $\{u_1, \dots, u_j, \dots, u_M\}$. These velocities are the candidates for the next velocity.
4. For each candidate velocity (bin) u_j make a set of window velocity pairs by adding the candidate velocity to the existing reference velocity set. The new reference velocity window pair sets which would be used in equation (9) is

$$\{v_1, \dots, v_N, u_j\}, \{\Omega_1, \dots, \Omega_{N+1}\}.$$

5. Choose a new reference velocity based on minimizing an error criterion between the known velocity function and the window velocity pairs.
6. Repeat until the error criterion is met.

It is not claimed that the algorithm produces optimal results but it does give good approximations to the velocity model for a given error. Figure 5 compares the approximations from the sequential process of building the velocity model for 4, 8, and 12 reference velocities.

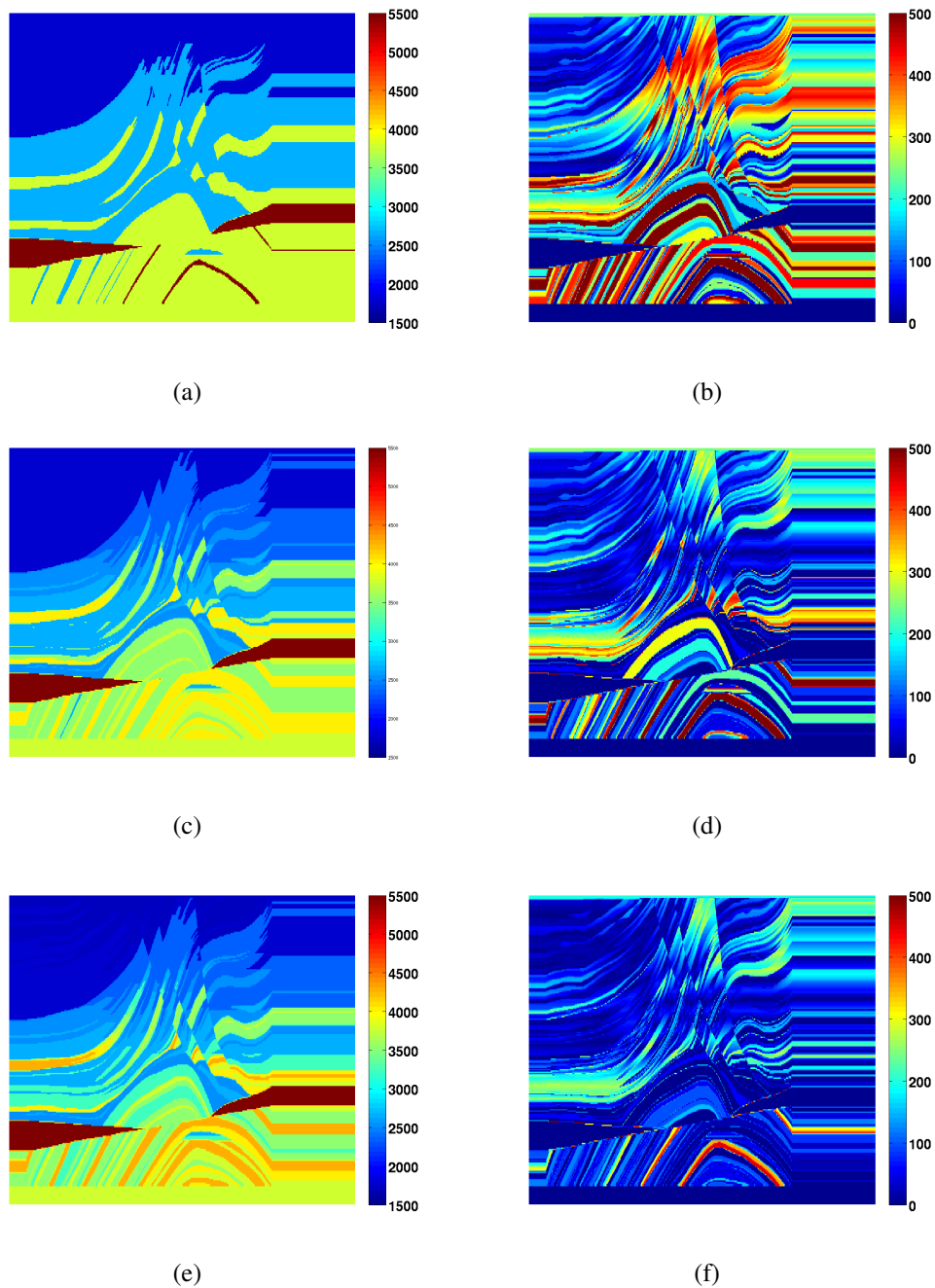


FIG. 5. Images (a),(c), and (e) are piecewise constant approximations of the velocity using 4, 8, and 12 reference velocities with mean error of 240m/s, 120m/s, 84m/s, respectively. Images (b),(d), and (f) are the plot of the absolute error between the approximations (a),(b), and (e), and the true velocity model, respectively. The units on the color bars of both types of images are m/s. For comparison, 18 reference velocities were used for the migration in Figure 6.

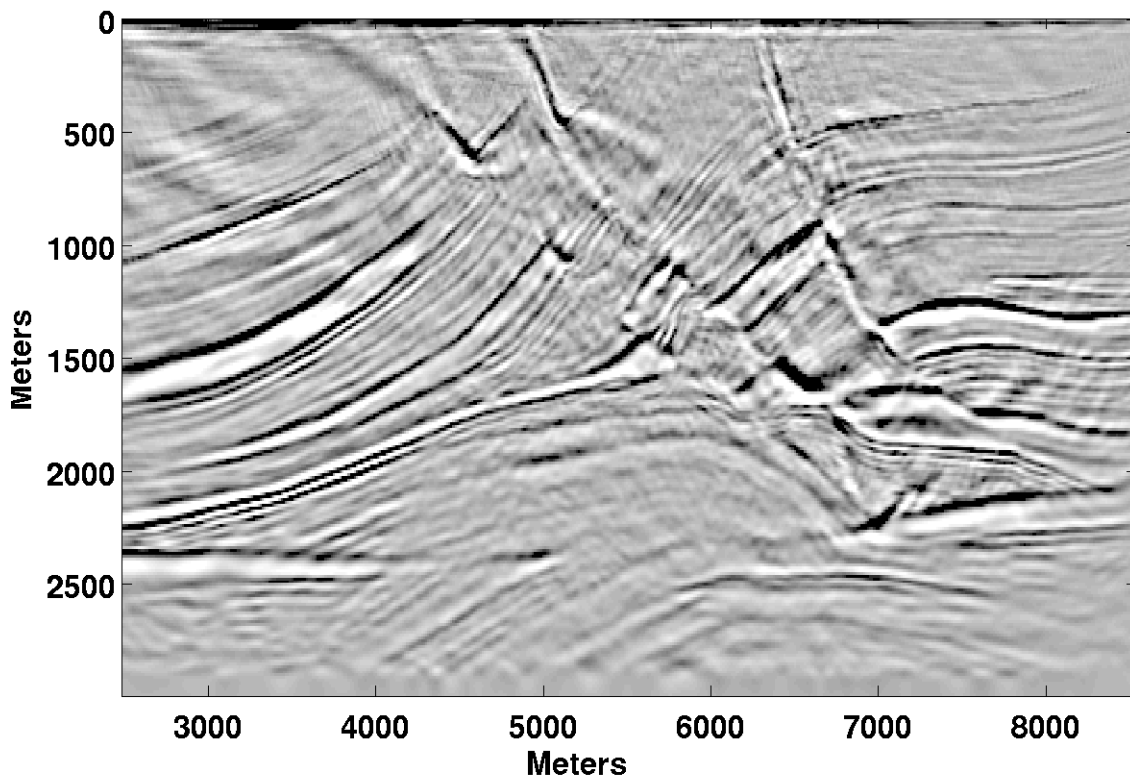


FIG. 6. An image the Marmousi data set using PSTS RTM. The run time for migrating a shot record is 12 minutes. The time step was 0.0015 ms, and the grid spacing was 12.5 m. An error criterion was used (40m/s) which produced 18 reference velocities.

THE MARMOUSI DATA SET

The Marmousi data set (Versteeg, 1994) is a common benchmark to test migration algorithms. Although it does not show the strengths of RTM, that is imaging overturned reflectors, it does demonstrate that PSTS RTM can image seismic data in a complex medium.

To benchmark PSTS RTM we compare it to a second order time and fourth order space finite-difference RTM. Figure 6 is the PSTS result and Figure 7 is the FD result. The FD RTM appears to be of higher quality. This is thought to be because of artifacts associated with a lower sample rate in the imaging condition. The FD image took twice as much time to calculate.

CONCLUSION

We proposed a Fourier domain time-stepping equation for RTM which is used to migrate the Marmousi data set. Our method multiplies the spatial Fourier transform of the wavefield by a cosine whose argument depends on velocity and wavenumber. This can be interpreted as a spatial phase shift. For comparison, the Marmousi dataset was migrated by finite-differencing the full wave equation. The two images were comparable in quality and the phase-shift time-stepping equation was computed in half the time. As a result of computing the phase shift time-stepping equation in the Fourier domain, a much larger time

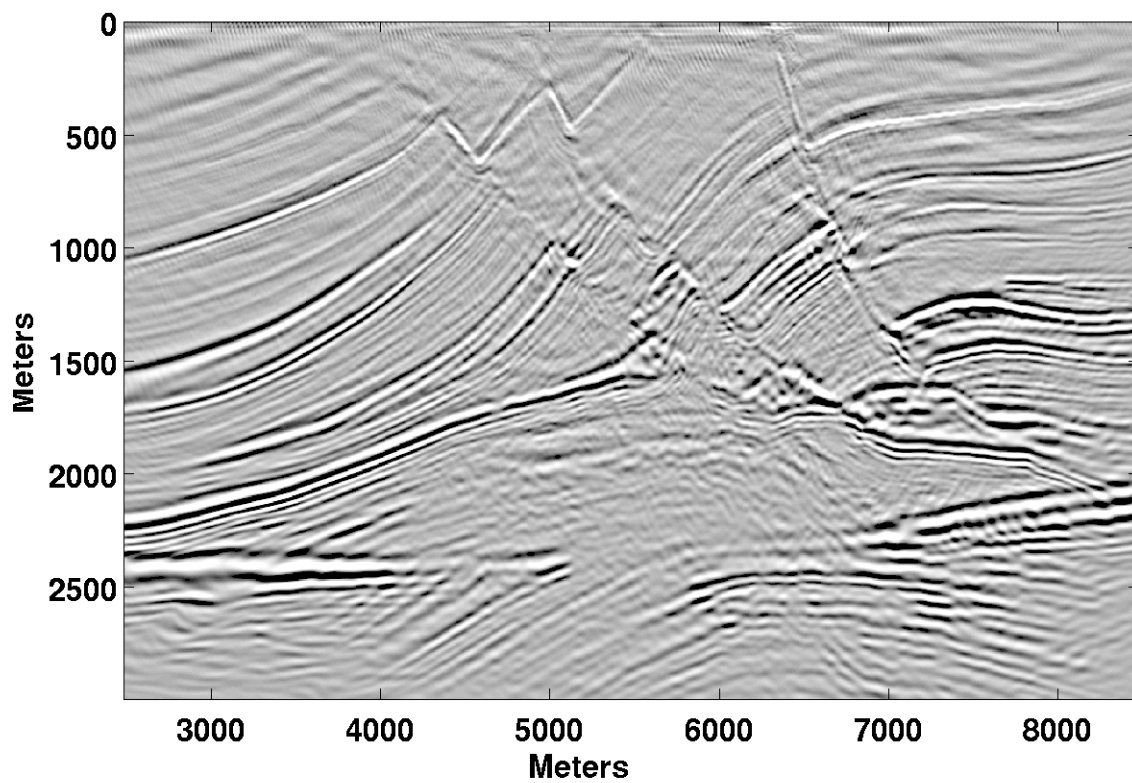


FIG. 7. An image of the Marmousi data set using second order time and fourth order space explicit finite difference RTM. The run time for migrating a single shot record is 24 minutes. The time step was 0.0003s and the grid spacing was 5m.

step is possible then by using finite-differences.

ACKNOWLEDGEMENTS

We thank the sponsors of the CREWES project, and those of the POTSI consortium, and especially NSERC, MITACS, PIMS, and Alberta Ingenuity.

REFERENCES

- Baysal, E., D. D. Kosloff, and J. W. C. Sherwood, 1983, Reverse time migration: *Geophysics*, **48**, 1514–1524.
- Candès, E., L. Demanet, and L. Ying, 2007, Fast computation of fourier integral operators: *SIAM J. Sci. Comput.*, **29**, 2464–2493.
- Gabor, D., 1946, Theory of communication: *Journal of the Institute of Electrical Engineers*, **93**, 429–457.
- Gazdag, J., 1978, Wave equation migration with the phase-shift method: *Geophysics*, **43**, 1342–1351.
- Grossman, J., G. Margrave, and M. P. Lamoureux, 2002, Constructing adaptive, nonuniform gabor frames from partitions of unity: CREWES Research Report 14.
- Jones, I. F., M. C. Goodwin, I. D. Berranger, H. Zhou, and P. A. Farmer, 2007, Application of anisotropic 3d reverse time migration to complex north sea imaging: *SEG Technical Program Expanded Abstracts*, **26**, 2140–2144.
- Ma, Y. and G. F. Margrave, 2008, Seismic depth imaging with the gabor transform: *Geophysics*, **73**, S91–S97.
- Margrave, G. and M. Lamoureux, 2002, Gabor deconvolution: CSEG annual mtg., Expanded Abstract.
- Margrave, G. F., 1998, Theory of nonstationary linear filtering in the fourier domain with application to time-variant filtering: *Geophysics*, **63**, 244–259.
- Margrave, G. F., P. C. Gibson, J. P. Grossman, D. C. Henley, V. Iliescu, and M. P. Lamoureux, 2005, The gabor transform, pseudodifferential operators, and seismic deconvolution: *Integr. Comput.-Aided Eng.*, **12**, 43–55.
- McMechan, G. A., 1983, Migration by extrapolation of time-dependent boundary values: *Geophysical Prospecting*, **31**, 413–420.
- Stein, E., 1993, *Harmonic analysis : real-variable methods, orthogonality, and oscillatory integrals*: Princeton University Press.
- Stolt, R. H., 1978, Migration by fourier transform: *Geophysics*, **43**, 23–48.
- Versteeg, R., 1994, The Marmousi experience; velocity model determination on a synthetic complex data set: *The Leading Edge*, **13**, 927–936.